Reports of CFRL (*Cold Fusion Research Laboratory*), **11-5**, pp. 1 – 14 (January, 2011)

Precision Measurement of Excess Energy in Electrolytic System Pd/D/H_2SO_4 and Inverse-Power Distribution of Energy Pulses vs. Excess Energy+

H. Kozima[1,2], W.-S. Zhang[2,3], and J. Dash[2]

[1]Cold Fusion Research Laboratory, 597-16 Yatsu, Aoi, Shizuoka 421-1202, Japan
E-mail: hjrfq930@ybb.ne.jp

[2] Low Energy Nuclear Laboratory, Portland State University, Portland, OR 97207-0751, U.S.A.,

[3] Institute of Chemistry, Chinese Academy of Sciences, P.O. Box 2709, Beijing 100080, China

+This paper is an extended version of the paper with the same title published in *Proc. ICCF13* (June 25 – July 1, 2007, Dagomys, Sochi, Russia) pp. 348 – 358 (2008).

Abstract

Excess energy was measured with a Seebeck envelope calorimeter in an electrolytic system containing a 2 mm diameter Pd tube cathode. After about 50 hours of electrolysis, many power pulses (P_{ex} < ~0.5 W) and bursts (P_{ex} > ~0.5 W) of excess power P_{ex} were observed. The distribution of the number of power pulses $N(P_{ex})$ with definite excess power P_{ex} plotted on a logarithmic scale is expressed as a straight line with a gradient ~ – 2 for P_{ex} < ~0.5 W showing the typical behavior of the $1/f$ noise. The distribution for P_{ex} > ~0.5 W deviates from this regularity. These characteristic behaviors are discussed in relation to complexity in the mechanism of the excess energy generation in the experimental system.

1. Introduction

There are several problems in the cold fusion phenomenon (CFP) which make it difficult for scientists to accept. The most important problem is the irreproducibility of experimental results. There are many examples, especially in nuclear physics, where events are governed by probabilistic law; decay of a radioactive nuclide and collision of

a particle with a group of other particles are the most common examples. Therefore, we have to be satisfied with statistical or qualitative reproducibility in such processes occurring in the CFP.

A second problem might be the mental threshold necessary to accept the idea that some kinds of nuclear reactions occur in solids differently from those in free space. At the center of this problem, there is the idea that the probabilities of nuclear fusions (especially *d*-*d* fusion) in solids become many orders (several tens of orders) of magnitude higher than in vacuum. This point might be at the core of the controversy between proponents and skeptical scientists since the report of the CFP in 1989 [1].

There are some hundreds of positive CFP experimental data sets obtained during the past 18 years, ranging from emission of particles, including neutrons, protons, tritons, and alpha particles, beta and gamma rays, to the generation of almost all light and heavy nuclei in the periodic table. Each element generated is accompanied by excess energy. These data sets are very complicated in their nature, as we see above from the list of products. The systems producing them are also complicated in their materials and methods.

To find a key to reconcile these complicated experimental data sets within the framework of modern physics, we have investigated the CFP phenomenologically at first [2] and then quantum mechanically, based on clues obtained from the data sets [3, 4].

The second point discussed above has a secret in itself. If nuclear reactions occur only between charged particles, it is apparent that such nuclear reactions could not be much different in vacuum than in solids due to the shortness of the nuclear force range of about 1 fm (= 10^{-15} m) compared with lattice constants of solids of about 1 Å (=10^{-10} m) as discussed in our paper and book [3, 4]. But the secret is a role of the neutron. In the experimental data sets, there are several showing important roles of neutrons. If experiments were performed in environments where no thermal neutrons exist, the CFP did not occur [5]. If experiments were done with artificial thermal neutron sources, the CFP were intensified [6].

Thus, it is natural to assume that thermal neutrons play some role in catalyzing the CFP. The model (TNCF model) including the so-called trapped neutrons in materials has been successfully applied to many experimental data sets with only one parameter to consistently explain observed results. Natural extension of this model should be a quantum mechanical verification of the premises used in the model as preliminary results have shown in recent reports [3, 4].

The first point discussed above has a somewhat different nature. There is no

question that a many-body system gives values of observables (physical properties) as averages over many constituent particles, in general. This is not appropriate for an observable which is measured individually not as an average. A nuclear reaction in solids is such a case where we measure reaction products individually; e.g. emission of neutrons (or other particles) is an example and excess energy pulses are another, if time resolution is fine enough to discriminate among different pulses. Then, the distribution of pulses against the strength of them will obey an inverse-power law, as many phenomena in many-body complex systems such as earthquakes [7], undersea ocean currents [8] and intensities of light from some astronomical sources [8].

Thus, it is possible to confirm the complexity of the CFP by checking the intensity distribution of excess energy pulses and their natural irreproducibility. Fortunately, there are a few systematic data sets of excess energy generation. Extensive experimental data by McKubre et al. [9] were roughly analyzed and the results showed inverse proportionality. [4]

In this paper, we analyze experiments obtained in the Low Energy Nuclear Laboratory (LENL), Portland State University using a Seebeck envelope calorimeter (SEC), and we show that the excess energy pulses obey the inverse power law. Also, that there appears a peculiar behavior in high energy pulses (bursts), suggesting the existence of a positive feed-back mechanism. These results will be discussed in relation to complexity.

2. Experimental

We used a closed cell (Fig.1), similar to that used before [10, 11] except that the height is less in order to fit into the Seebeck envelope calorimeter SEC. The electrolytic cell is a Pyrex cylinder (capacity is about 280 ml, ϕ_{in} = 50.7 mm and ϕ_{out} = 57.0 mm, wall thickness = 3.2 mm, h = 142 mm). A PTFE female top cap has ϕ_{out} = 65 mm and ϕ_{in} = 57 mm; it has two 1mm diameter holes for the electrode lead wires. A PTFE plate (ϕ 50 mm) with many 0.8 mm holes, which also has two 1 mm diameter holes for the electrode lead wires, is used for suspending recombination catalyst above the electrode. A PTFE rod fastened to the perforated plate and the top cap serves to suspend the catalyst a fixed distance above the electrolyte.

A gasket made of ethylene propylene (resistant to sulfuric acid) is used to seal the top cap against the top edge of the Pyrex cylinder.

The Pd cathode is a 80 mm long palladium tube, ϕ_{out} = 1.67 mm, ϕ_{in} = 0.67 mm, The upper 50 mm of the Pd cathode is sealed against the Pt lead wire with heat-shrunk PTFE tubing. The platinum anode is a U-shaped foil 37.5 × 23.8 × 0.12 mm^3. The Pt anode

lead wire is crimped to the anode foil. The anode lead wire is also encased in heat-shrunk PTFE tubing.

The electrolyte is heavy water (99.9 at.%, Aldrich catalog #347167) mixed with 96.4% H_2SO_4 (J.T. Baker, Lot # K10030) in the volume ratio of 6.7:1.

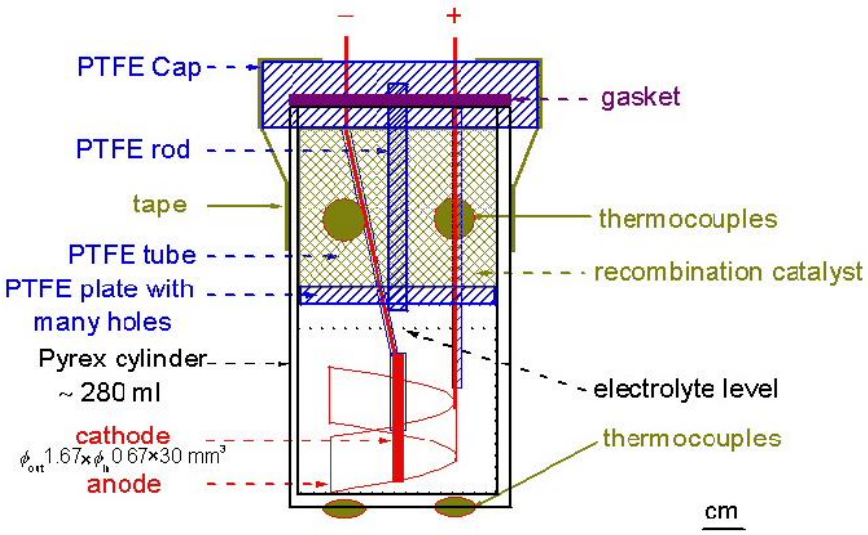

Fig. 1. Cell with Pd tube cathode and Pt foil anode which was used for electrolysis.

3. Experimental results and discussion

The size of the Pd tube cathode is the same as that used by Zhang et al. [12]: dimensions are 0.67ϕ × 1.67ϕ × 80 mm^3, but only the lower 30mm of the Pd tube was exposed to electrolyte.

Using this value we obtain following numerical data about the Pd cathode; Surface area $S = 3 \times \pi\ (0.067 + 0.167)\ cm^2 = 2.21\ cm^2$, Effective volume V_{eff} (assuming a thickness of 1 micrometer at the surface);

$V_{eff} = 10^{-4}\ S = 2.21 \times 10^{-4}\ cm^3$.

According to the TNCF model [4] (assuming only the CF version of the $n + d$ reaction) and thermalization of the liberated energy in the sample,

$n + d = t\ (6.98\ keV) + Q\ (6.25\ MeV)$. (1)

The number of reactions N in time τ is given as follows [2 – 4]:

$N = 0.35\ n_n v_n n_d V \sigma_{nd} \tau$ (2)

where $0.35 n_n v_n$ is the flow density of the trapped thermal neutrons per unit area and time, n_d is the density of deuterons, $\sigma_{nd} = 5.5 \times 10^{-28}\ cm^2$ is the cross section of the

reaction (1) for a thermal neutron..

The number of reactions N is related to the number of reactions N_Q producing excess energy Q (in MeV) defined by a relation

$N_Q = Q$ (MeV)/5 (MeV),

if we assume the energy liberated in a nuclear reaction is on average 5 MeV (actually, the energy is 6.25 MeV if we assume only the reaction (1)).

Putting

$n_d = 6.88 \times 10^{22}$ cm^{-3}

for the sample composition PdD, and the neutron velocity

$v_n = 2.2 \times 10^5$ cm/s

for the thermal neutron in (2), we can calculate the parameter n_n, density of trapped neutrons, in the TNCF model using the observed excess energy Q in a time τ. The value n_n is given as follows if we assume $N = N_Q$:

$n_n = (\alpha_w /5)(1/0.35 v_n n_d V_{eff} \sigma_{nd} \tau)$,

where a parameter α_w is defined for convenience in the following discussion as

$\alpha_w = Q /\tau$,

which gives the excess thermal power in watts. The parameter α_w in watt (W) is also expressed by α in MeV/s as

$\alpha_w = 6.24 \times 10^{12}\ \alpha$ (MeV/s).

Using numerical values given above and also $\tau = 1$ (s) in the above relation, we obtain the final result

$$n_n = 7.2 \times 10^{15}\ \alpha_w\ (\text{cm}^{-3}). \qquad (3)$$

3,1 Experimental data;

Case 1. Active period with excess power pulses in the LENL data.

In the experimental data sets obtained in LENL, there are active periods with many excess power pulses generating excess power of about $\alpha_w = 0.1 – 0.2$ W. In these periods, we take $\alpha_w = 0.1$ W for analysis, for simplicity.

Then, we obtain the density of the trapped neutrons from formula (3);

$$n_n = 7.2 \times 10^{14}\ (\text{cm}^{-3}). \qquad (4)$$

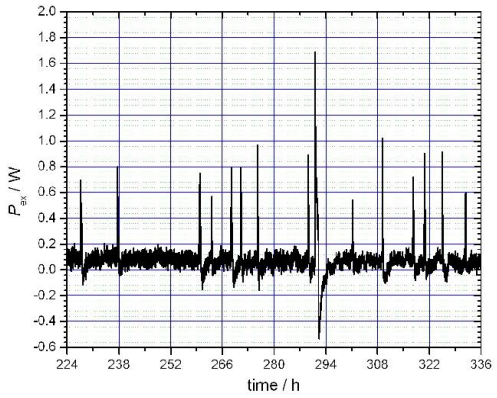

Fig. 2. Excess power pulses and bursts during a 112 hour period of an experiment (061026) which lasted 14 days as a whole.

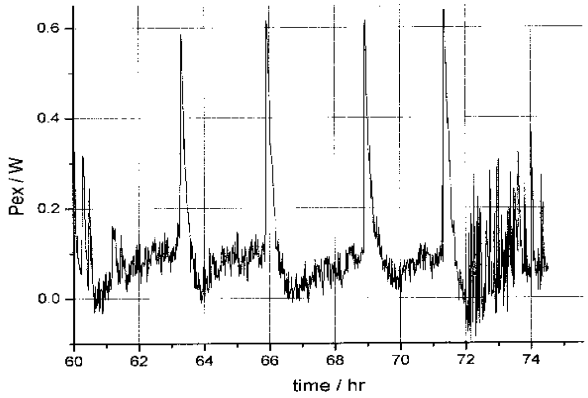

Fig. 3. Excess power pulses during a 14 hour period of an experiment (070108) which lasted 12 days as a whole.

Case 2. Bursts in the LENL data.

In the experimental data sets obtained in LENL, there are excess power pulses and bursts (rather large pulses than 0.5 W) up to 2 watts. Some of these bursts are shown in Figs. 2 and 3.

During most of the experiment the excess power was about 0.1±0.1 W. Most of the large bursts were less than 1 W, but there was one burst which reached 2 W. Following each large burst, the SEC recorded negative power. It is possible that recombination power was lost due to increase in gas pressure in the cell when the power burst occurred. The O-ring seal at the top of the cell is not rigid. Therefore, an increase in gas pressure inside the cell could cause an increase in the rate of escape of recombination gases, thus reducing the temperature in the space occupied by the recombination catalyst.

For the cases of bursts (0.5 W $\leq P_{ex} \leq$ 2 W), we take α_w = 2 W for analysis, for simplicity.

Then, the density of the trapped neutrons (3) for the bursts is given as

$n_n = 7.2 \times 10^{16}$ (cm^{-3}). (5)

Case 3. Experiment of Zhang et al. [12]

In this experiment with an explosion as explained in their paper [12], we can assume the excess power of

$P_{ex} = 1.9 \times 10^5$ W.

This means that the parameter α_w defined above is given as $\alpha_w = 1.9 \times 10^5$ W and we obtain the value of the parameter (3) for the explosion as

$n_n = 1.4 \times 10^{20}$ (cm^{-3}). (6)

3.2 Discussion

In our analyses obtained until 1998 and published as a book [2, 4], we determined the parameter n_n for more than 60 experimental data sets giving values between $10^8 - 10^{13}$ cm^{-3};

$n_n = 10^8 - 10^{13}$ cm^{-3}. (7)

It is interesting to compare the value of the parameter n_n given in the relation (7) with the values (4) – (6) determined in the above Cases. The experimental data given in the Case 1 have the parameter (4) in the range given in (7). On the other hand, the parameters (5) and (6) of the Cases 2 and 3 are the largest values of n_n, exceeding the range expressed in the relation (7).

These large values of the parameter n_n in Cases 2 and 3 show, of course, the large value of the excess energy in a reduced form, making it easy to compare the intensities of the reactions. Then, we have to discriminate the latter cases (Cases 2 and 3) from such “normal” events in the CFP as the Case 1 giving the value n_n in the relation (7).

This characteristic feature of Case 2 (and Case 3) is also shown by plotting a N_P vs. P_{ex} diagram, where N_P is the frequency of a definite excess power evolution P_{ex} such as given in Fig. 2.13 of [4] for the data by McKubre et al. [9].

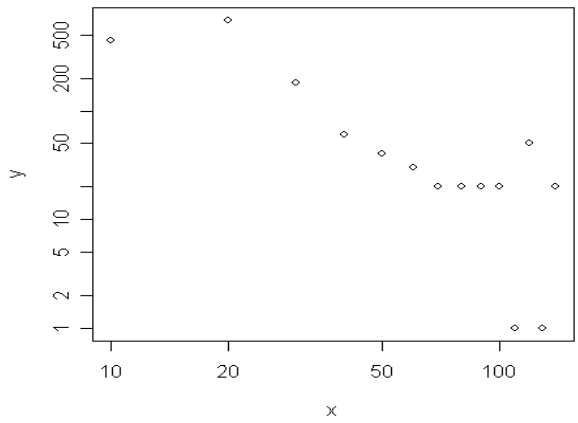

Fig. 4. Distribution of the frequency N_P (= y) producing excess power P_{ex} (= x). To depict log-log curve, values of N_P and P_{ex} were arbitrarily multiplied by 10^n. (x = 100 in this figure corresponds to P_{ex} = 1 W)

The corresponding figure in the case of the data sets obtained in LENL (including Cases 1 and 2) is depicted in Fig. 4. Data points were counted from excess power peaks (about 250 pulses and bursts) in such diagrams as Figs. 2 and 3 in the following time periods in three runs; 1) time period 86.8 – 88.4 hours of run #060620, 2) time period 3 – 12 hours of run #061007, 3) time period 22 – 90 hours of run #070108.

Figure 4 shows following facts (x = 100 correspond to P_{ex} = 1 W in this figure):

Region A, x = 20 – 60.

The data points in the range from x = 20 to 60 are considered to be on a straight line with a gradient ≈ – 2.

This value of the gradient ≈ – 2 is compared with the value ≈ – 1 [4] obtained for the data by McKubre et al. [9]. These values for two data sets may depend on characteristics of the cathodes used in the experiments, if we consider the Gutenberg-Richter law of earthquakes, discussed above. In the case of the earthquakes, it is said that the exponent (≈ –1.7) of the inverse-power law depends on location, and it fluctuates with time [7].

Region B, x > 60.

The data points in the range x > 60 deviate from the straight line. Some points are very low and some very high above the extrapolated straight line from Region A.

The data in region A is similar to the data depicted in the Fig. 2.13 [4] for the data obtained by McKubre et al. [9], but it has a different gradient. On the contrary, the data

in region B has a different characteristic and should be analyzed with different factors from those used in the case of the data in region A.

One possible explanation for the difference in characteristics of the data in region B and those in region A is in the behavior of complex systems with nonlinear interaction resulting in self-organization and chaos. We may imagine the following processes 1) – 3).

1) If the temperature of the experimental system is lower than a critical temperature T_c (from the experiment, we may take it higher than 60 degC; $T_c \geq 60$ degC), there are no cold fusion reactions.

2) Increasing the temperature higher than T_c (T_c < 90 degC as confirmed by experiments), the cold fusion reactions start to occur and produce excess energy inducing more reactions as we see in the occurrence of many pulses.

This means that the critical temperature T_c in this case is in between 60 and 90 degC (60 degC $\leqq T_c \leqq$ 90 degC).

3) We may assume that higher temperature is more favorable for the CFP if other conditions are the same. Then, when the temperature of the sample increases due to CF reactions generating more excess energy than dissipating energy from the system and the shape of the tubular cathode is favorable of the positive feedback of the CFP, there may occur a positive feedback which increases the temperature of the system, thus inducing more CF reactions.

This positive feedback results in the excess energy bursts as seen in region B. When the cycle of the positive feedback last long, there may appear negative feedbacks due to changes of other parameters (e.g. decrease of D/Pd ratio, change of lattice structure, changes in surface composition, etc.) to over -compensate the positive feedback and reduce the sample temperature.

The explosions observed by Zhang et al. [12] and also by Biberian [13], both of whom used tubular Pd cathodes, might be the extreme examples of this positive feed-back when the negative feedback did not work well to prevent the explosions. The other explosions experienced by Fleischmann et al. [1] and Mizuno et al. [14] may be explained by similar processes.

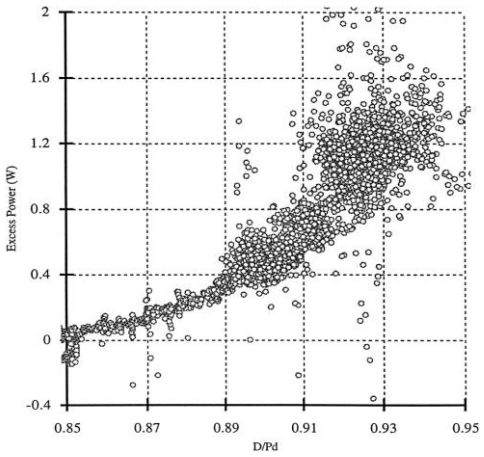

Fig. 5. Variation of excess power with loading ratio D/Pd obtained by McKubre et al. [9].

A similar figure was obtained by McKubre et al. [9] for the dependence of P_{ex} on D/Pd ratio as reproduced in Fig. 5.

Figure 6 shows the classic graph (Fig. 7) of the evolution of the final equilibrium states of the logistic difference equation (l.d.e.), well-known in the field of complexity [15].

We see a bifurcation in Fig. 4 similar to that of the state into “Period two” in Fig. 6 of l.d.e.

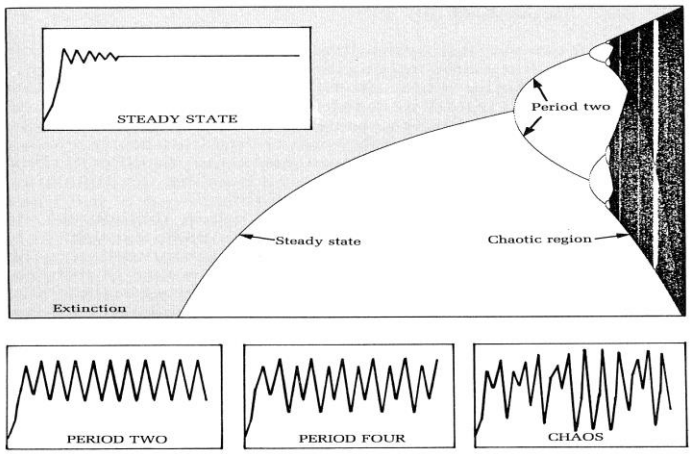

Fig. 6. Bifurcation diagram to show period-doubling and chaos (From “Chaos” by J. Gleick [15]. p.71). The main figure depicts x_∞ (ordinate, x_n at $n = \infty$) vs. the parameter λ(abscissa) of the logistic difference equation, i.e. l.d.e., $x_{n+1} = \lambda x_n(1 - x_n)$ $(0 < x_0 < 1)$. The inserted figures, a) Steady state, b) Period two, c) period four, and d) chaos, depict variations of x_n with increase of suffix n (temporal variation if n increases with time) for four values of λ; a) $1 < \lambda < 3$, b) $3 < \lambda < 3.4$, c) $\lambda \simeq 3.7$, d) $4 < \lambda$. The region a), b) and d) correspond to “Steady state”, “Period two” and “Chaotic region” in the

main figure, respectively.

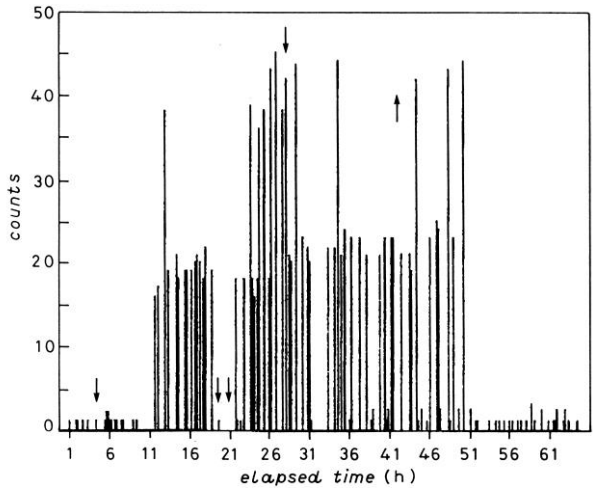

Fig. 7. Diagram showing the time evolution of the neutron emission counts (ordinate) during the first run (7-10 April, 1989) by De Ninno et al. [16]. The values indicated are integral counts over periods of 10 minutes.

Temporal evolution of the excess power generation depicted in Figs. 2 and 3 also shows the time dependence of excess power similar to those of l.d.e. depicted in the inserted figures “Chaos” and “Period four” in Fig. 6.

The dispersion of experimental data points in Fig. 5 obtained by McKubre et al. [9] may be the manifestation of chaos appeared in l.d.e. shown in the rightmost part of Fig. 6.

It is possible to add another example of the bifurcation-like behavior in the temporal evolution of the CFP in the neutron emission as shown in Fig. 7 [16]. In this figure, the number of neutron counts is plotted on the ordinate as integral values over periods of 10 minutes. This does not necessarily reproduce faithfully the microscopic processes occurring in the sample. The figure shows, however, similar characteristics to those appearing in the data of excess power production obtained in LENL such as the bifurcation and the positive feedback of the CFP shown in Figs. 2 and 3.

It is noticed in the experiment by De Ninno et al. [16] that parameters (T, η = D/Ti ratio, etc.) were varied by cycling change of temperature between 77 K and the room temperature.

At present, we have only an analogy between the data sets of the CFP and the complexity depicted by the l.d.e. Though we have shown only three experimental data

sets by Dash et al., McKubre et al. [9] and De Ninno et al. [16], there are many data sets in the CFP showing characteristics common in complexity.

4. Conclusion

Almost all CF systems satisfy the sufficient conditions for the occurrence of complexity which is common in any nonintegrable system with Poincaré resonances (both in classical and quantum mechanics), according to the definition by I. Prigogine [17]. That is, they are open, non-equilibrium (far– from- equilibrium), many body systems with non-linear interactions between components.

In addition to this general nature of CF systems, we have many experimental data sets in the CFP that show characteristics of many-body systems and complexity. The most outstanding examples of them are the two laws we have found before, that show many-body effects of the CFP;

(1) **The first law**; The Inverse-Power Law of $N(P_{ex})$ vs. P_{ex} Relation, where $N(P_{ex})$ is the number of events producing excess power P_{ex} ([4] §2.12 and Fig. 1) and

(2) **The second law**; The Stability Effect in the Yield of Product Elements by nuclear transmutation ([4] §2.11).

The third law described in this paper shows the chaotic nature of the CFP, i.e.

(3) **The third law**; The Bifurcation and Chaos of the Cold Fusion Phenomenon in the occurrences of excess energy (Figs. 2, 3, 4 and 5) and neutron emission (Fig. 7).

The last law shown in this paper by comparison with the l.d.e. may be legitimated by a discovery by Feigenbaum that “there are certain universal laws governing the transition from regular to chaotic behavior, roughly speaking, completely different systems can go chaotic in the same way [18].

Another characteristic we could notice from Fig. 4, depicted by data analysis from the point of view of the inverse-power law, is the appearance of positive feedback in reactions participating in the CFP. This point of view gives us a consistent perspective that makes it possible to understand such various heterogeneous data sets in this field as null results, e.g. [5], small and large pulses of excess power (e.g. Figs. 2 and 3) and neutron emission (e.g. [18]), and explosions [1, 12 – 14].

From the specification of CF systems sufficient to expect characteristics of the stochastic processes and complexity to occur in them and the three laws (or regularities) found in the CFP as described above, we understand that the CFP is a phenomenon governed by probabilistic laws and complexity. Therefore, investigation of the CFP should be performed realizing its nature of the open, non-equilibrium system composed of many components combined together with nonlinear interactions. Many

controversies surrounding the CFP can be resolved by our realization of its nature. New developments may be expected if we establish the science of the cold fusion phenomenon.

We have to realize also that our knowledge in natural science is not complete. There remain unexplored research fields in physics such as halo nuclei with medium mass numbers and also wavefunctions of occluded protons/deuterons in fcc/hcp transition metals. These properties of exotic nuclei and protons/deuterons wavefunctions may be closely related to the occurrence of the CFP, as we have explored a few steps already as reported in [3, 4].

Acknowledgment

This work is supported by a grant from the New York Community Trust.

References

1. M. Fleischmann, S. Pons and M. Hawkins, "Electrochemically induced Nuclear Fusion of Deuterium," *J. Electroanal. Chem*., **261**, 301 – 308 (1989).

2. H. Kozima, *Discovery of the Cold Fusion Phenomenon*, Ohtake Shuppan, Tokyo, 1998. ISBN: 4-87186-044-2.

3. H. Kozima, "Quantum Physics of Cold Fusion Phenomenon," in *Developments in Quantum Physics*, eds. K. Krasnoholovets and F. Columbus, Nova Science Publishers, Inc. 2004. ISBN: 1-59454-003-9. And also H. Kozima, *Rep. Fac. Science, Shizuoka Univ.* **39**, 21 – 90 (2005).

4. H. Kozima, *The Science of the Cold Fusion Phenomenon*, Elsevier Science, London, 2006. ISBN-10: 0-08-045110-1

5 For instance, S.E. Jones, D.E. Jones, D.S. Shelton and S.F. Taylor, "Search for Neutron, Gamma and X-Ray Emission form Pd./LiOD Electrolytic Cells: A Null Results," *Trans. Fusion Technol*. **26**, 143 (1994).

6. For instance, B. Stella, M. Corradi, F. Ferrarotto, V. Milone, F. Celani and A. Spallone, "Evidence for Stimulated Emission of Neutrons in Deuterated Palladium," *Proc. ICCF3*, p. 437 (1993)

7. For instance, L. Anton, "Simple equation for earthquake distribution" *Phys. Rev*. **E59**, 7213 – 7215 (1999). And also B. Gutenberg and C.F. Richter, *Ann. Geophys*. (C.N.R.S.) **9**, 1 (1956).

8. W.H. Press, "Flicker Noises in Astronomy and Elsewhere," *Comments Astrophys*. **7**, 103 – 119 (1978)

9. M.C.H. McKubre, S. Crouch-Baker, Riley, S.I. Smedley and F.L. Tanzella, "Excess

Power Observed in Electrochemical Studies of the D/Pd System," *Proc. ICCF3* , pp. 5 – 19 (1993).
10. W.-S. Zhang, J. Dash and Q. Wang, "Seebeck Envelop Calorimetry with a Pd/D_2O + H_2SO_4 Electrolytic Cell," *Proc. ICCF12,* pp. 86 – 96 (2006).
11. W.-S. Zhang and J. Dash, Excess Heat Reproducibility and Evidence of Anomalous Elements after Electrolysis in Pd/ Pd/D_2O + H_2SO_4 Electrolytic Cell" *Proc. ICCF13* (to be published)
12. X. Zhang, W-S. Zhang, D. Wang, S. Chen, Y. Fu, D. Fan and W. Chen, "On the Explosion in a Deuterium/Palladium Electrolytic System, "*Proc. ICCF3,* p. 381 (1992).
13. J.-P. Biberian, "Explosion during an electrolysis experiment in an open cell mass flow calorimeter," presented at *6th International Workshop on Anomalities in Hydrogen/Deuterium loaded Metals,* Siena, Italy, May 13-15 2005.
14. T. Mizuno and Toriyabe, "Anomalous energy generation during conventional electrolysis" *Proceedings of ICCF12,* pp. 65 – 74, (2006)
15. J. Gleick, *Chaos*, Penguin books, ISBN 0-14-00.9250-1
16. A. De Ninno, A. Frattolillo, G. Lollobattista, G. Martinio, M. Martone, M. Mori, S. Podda and F. Scaramuzzi, "Evidence of Emission of Neutrons from a Titanium-Deuterium System," *Europhys. Lett*. **9**, 221 (1989)
17. I. Prigogine, *The End of Certainty***,** The Free Press, New York, 1996. ISBN 0-684-83705-6
18. S.H. Strogatz, *Nonlinear Dynamics and Chaos*, p. 3, Westview Press, 1994. ISBN-10; 0-7382-0453-6.